First Crystallographic Investigation of Complexes of *cis*-VO_2^+, *cis*-MoO_2^{2+}, and *trans*-UO_2^{2+} Species with Schiff-Base Molecules Derived from 4,6-*O*-Ethylidene-β-D-glucopyranosylamine

Ajay K. Sah,[a] Chebrolu P. Rao,*[a] Pauli K. Saarenketo,[b] Elina K. Wegelius,[b] Erkki Kolehmainen,[b] and Kari Rissanen[b]

Dedicated to Professor Animesh Chakravorty, IACS, Calcutta, on the occasion of his 65th birthday

Keywords: Vanadium / Molybdenum / Uranium / Schiff bases / Structure elucidation

The interaction of Schiff-base ligands derived from 4,6-*O*-ethylidene-β-D-glucopyranosylamine with *cis*-VO_2^+, *cis*-MoO_2^{2+}, and *trans*-UO_2^{2+} species have been studied by isolating and characterizing the corresponding products. The structures of one complex of each type of species have been established by single-crystal X-ray diffraction analysis. In all the complexes, the saccharide moiety adopts a chair conformation and has a β-anomeric form. A gradual increase in coordination number (5, 6, and 7) and a gradual variation in the geometry (distorted trigonal-bipyramidal, distorted octahedral, and pentagonal-bipyramidal) are observed on going from the complexes of *cis*-VO_2^+ (mononuclear) to *cis*-MoO_2^{2+} (mononuclear) to *trans*-UO_2^{2+} (dinuclear). A variation in the binding mode of the ligand towards these dioxometal species is also observed. Intermolecular interactions of the type O–H···O, C–H···O, and N–H···O present in the lattices of these complexes lead to the formation of interesting structures.

Introduction

About two-thirds of the carbon in the biosphere is present in various forms of carbohydrates.[1] Carbohydrates not only act as the major source of energy for living beings, but also as building blocks for the formation of polysaccharides, nucleic acids, and antibiotics. The coexistence of saccharides and metal ions was established in the context of biological systems.[2] Although the metal ion−saccharide interactions were recognized long ago, the early literature was mainly concerned with solution studies, primarily with metal ions of the alkali and alkaline earth groups and of main group elements, as well as their adducts.[3] Only during the past decade have such interactions been delineated in the case of transition metal ions by isolation and characterization of the products.[4] In order to improve the binding affinities towards metal ions, as well as to isolate the metal ion−saccharide products in crystalline form, new strategies for saccharide modification have been developed. One such attempt of ours in this context recently resulted in the synthesis and characterization of complexes of *N*-(*o*-carboxyphenyl)-4,6-*O*-ethylidene-β-D-glucopyranosylamine with alkali and alkaline earth metal ions and the crystal structure of its potassium complex.[5] In this new strategy, the study of metal−saccharide interactions is attempted using the products of condensation of 4,6-*O*-ethylidene-β-D-glucopyranosylamine with salicylaldehyde and its derivatives as ligands suitable for metal ion binding. The results of these efforts are reported herein. Thus, the present studies are in continuation of our ongoing interest in establishing the interaction of OH-containing ligands with oxometal ion species, such as *cis*-VO_2^+, *cis*-MoO_2^{2+}, and *trans*-UO_2^{2+}. Studies of such oxometal ion species are also important with regard to the stereochemical preferences in binding to these new types of saccharide−Schiff-base ligands.

Therefore, we report herein the synthesis, characterization, and crystal structure determination of *cis*-VO_2^+, *cis*-MoO_2^{2+}, and *trans*-UO_2^{2+} metal ion complexes with salicylidene Schiff-base ligands derived from a glycosylamine, 4,6-*O*-ethylidene-β-D-glucopyranosylamine. The products have been characterized on the basis of their FT-IR- and NMR-spectroscopic data, FAB mass spectra, and single-crystal X-ray structural data. To the best of our knowledge, the three crystal structures of the saccharide−Schiff-base complexes of *cis*-VO_2^+, *cis*-MoO_2^{2+}, and *trans*-UO_2^{2+} reported herein are the first of their kind.

[a] Bioinorganic Laboratory, Department of Chemistry, Indian Institute of Technology Bombay,
Powai, Mumbai 400 076, India
Fax: (internat.) + 91-22/572-3480
E-mail: cprao@chem.iitb.ac.in
[b] Department of Chemistry, University of Jyväskylä,
40351 Jyväskylä, Finland
Supporting information for this article is available on the WWW under http://www.eurjic.com or from the author.

Results and Discussion

The ligands derived from 4,6-*O*-ethylidene-β-D-glucopyranosylamine and their complexes with dioxometal species of V, Mo, and U are shown in Scheme 1. While the reactions of *cis*-MoO_2^{2+} and *trans*-UO_2^{2+} gave the products in

  1434−1948/01/1111−2773 $ 17.50+.50/0

high yields, those with *cis*-VO_2^+ resulted in rather low yields. This is attributable to the formation of a second product in the case of the vanadium reactions, which could not be isolated in pure form. Evidence for this was provided by UV/Vis studies. The products with V and Mo were found to be mononuclear, while those with U were dinuclear. All exhibited a 1:1 metal-to-ligand ratio.

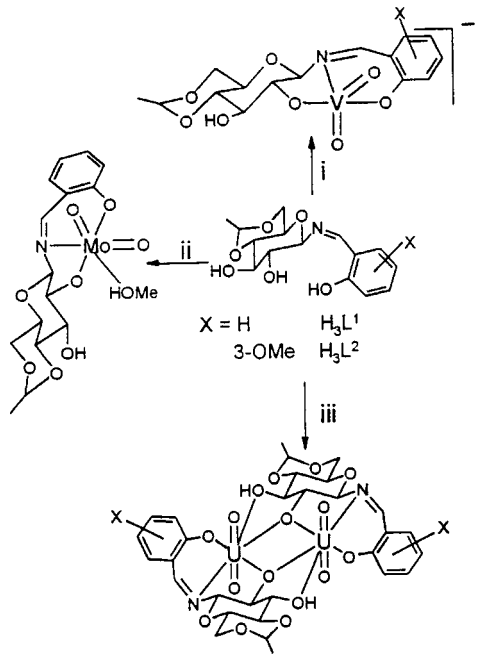

Scheme 1. Syntheses of the *cis*-VO_2^+, *cis*-MoO_2^{2+}, and *trans*-UO_2^{2+} complexes in methanol using the ligands $\mathbf{H_3L^1}$ and $\mathbf{H_3L^2}$: (i) $VO(acac)_2$, (ii) *cis*-$MoO_2(acac)_2$, and (iii) *trans*- $UO_2(OAc)_2{\cdot}2H_2O$

FT-IR

Comparison of the FT-IR spectra of all the complexes with those of their precursor ligands supported the formation of the respective complexes through the observation of substantial spectral changes. Characteristic vibrational bands corresponding to the M=O groups are observed for all the complexes. The ligand exhibits two distinct bands in the ν_{OH} region, whereas only one broad signal is observed for the corresponding complexes, indicating the loss of some hydroxy protons during complexation. This conclusion was further supported by the ^{1}H NMR spectra as well as by the crystal structure determinations. The ν_{OH} is generally shifted to higher frequencies by about 100 cm^{-1} for the uranium complexes as compared to the position of this band for their vanadium and molybdenum counterparts; this can be attributed to the fact that 3-OH is involved in metal ion binding in the former, whereas it is free in the latter.

^{1}H NMR

The spectra of all the complexes are indicative of the presence of a single anomeric form. However, upon addition of a small amount of D_2O to the respective solutions, spectral peaks corresponding to a second anomer appear with time. Upon complexation, only a single hydroxy proton signal remains in the alkyloxy region, indicating the loss of the phenolic and one of the alcoholic protons. The signals of the skeletal protons of the saccharide moiety are subject to an overall downfield shift upon complexation, this shift being more pronounced in the case of the uranium complex as compared to the vanadium and molybdenum complexes. Thus, the downfield shift of the signals of the skeletal protons is in the order *trans*-UO_2^{2+}complex >> *cis*-MoO_2^{2+} complex > *cis*-VO_2^+ complex. This may be attributed to the additional involvement of 3-OH (in addition to 2-OH) in the complexation in the case of the UO_2^{2+} species. The same trend was observed for the the HC=N and 1-H proton signals of the complexes. The $J_{C1\text{-}H}$ values were found to be 8.79 and 7.69 Hz for $VO_2(HL^1)$ and $VO_2(HL^2)$, respectively, supporting the presence of the saccharide moiety in the β-anomeric form.[16] The β-anomeric form of the saccharide moiety was unequivocally established on the basis of the crystal structures of the three complexes.

FAB MS

FAB MS studies supported the mononuclear nature of the V^V and Mo^{VI} complexes and the dinuclear nature of the U^{VI} complexes through exhibiting molecular ion peaks. Furthermore, the spectra of the vanadium complexes revealed the formation of the monooxo dinuclear species shown in Figure 1.

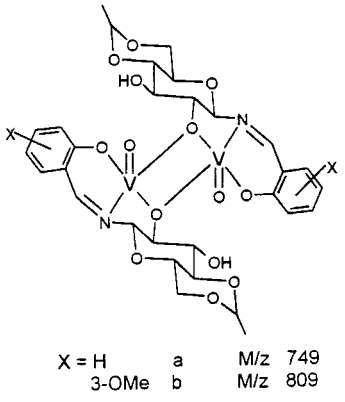

Figure 1. The dimeric species of monooxo V^V identified in the mass spectra

UV/Vis

Electronic spectra of all the complexes were recorded using freshly prepared solutions in DMSO at concentrations of 10^{-2} and 10^{-4} M; the corresponding spectra are shown in Figure 2. While the complexes of molybdenum and uranium (Figures 2b, 2c) proved to be stable in DMSO solution even after 36 h, those of vanadium underwent some cleavage and some free ligand was liberated (Figure 2a). An additional band was observed at 530−540 nm in the spectra, indicating the formation of some new oxovanadium species.

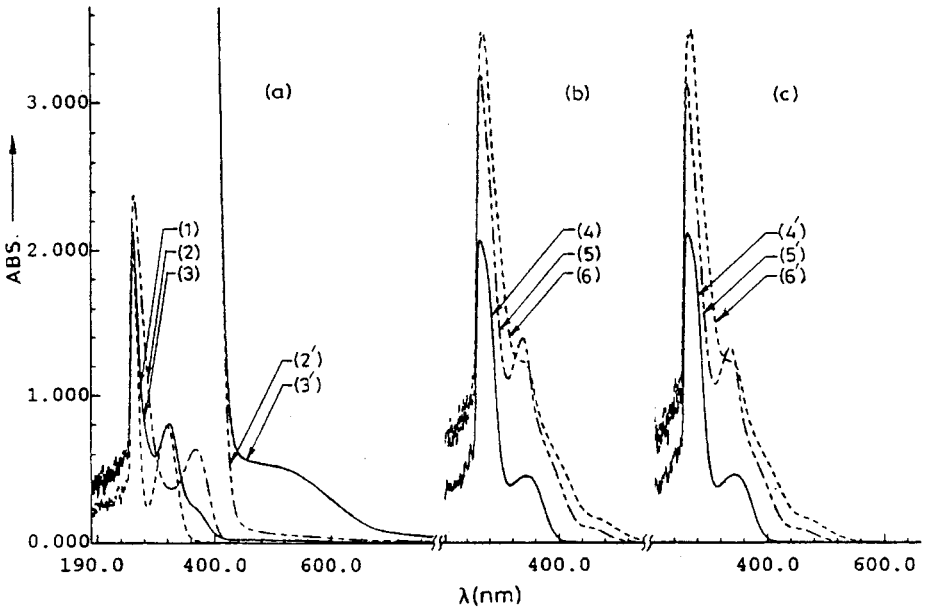

Figure 2. UV/Vis absorption spectra in DMSO: (a) spectrum (1) corresponds to H_3L^1, spectra (2, 2′) correspond to a freshly prepared solution of *cis*-$VO_2(HL^1)$, and spectra (3, 3′) correspond to the same complex analysed 36 h after dissolution; (b) and (c) spectra (4, 5, 6) correspond to freshly prepared solutions of the *cis*-$[MoO_2(HL^1)]$, *trans*-$[\{UO_2(HL^1)\}_2]$, and *trans*-$[\{UO_2(HL^1)\}_2]$ complexes, respectively, while spectra (4′, 5′, 6′) correspond to the same solutions after 36 h

Optical Rotation

The mononuclear complexes of *cis*-VO_2^+ and *cis*-MoO_2^{2+} showed a substantial change in specific rotation as compared with the specific rotations of the corresponding ligands.

Molecular and Crystal Structure of $VO_2(HL^1)$

Slow evaporation of the solvent from a concentrated methanolic solution of the complex resulted in single crystals in the monoclinic system. The crystal structure revealed the presence of a *cis*-dioxo mononuclear V^V complex, which is rather rare in vanadium−saccharide chemistry. Earlier reports dealt with either dioxo dinuclear homoleptic[7,8] or monooxo complexes of mixed ligands.[9] In the complex **$VO_2(HL^1)$**, the saccharide derivative is bound as a tridentate dianionic ligand, where 2-OH of the saccharide moiety extends coordination in its deprotonated form resulting in an ONO core, and where the other two ligations are extended by the salicylidene moiety. This results in the formation of one five- and one six-membered chelate. In order to compensate for the negative charge present on the complex, a dimethylammonium cation is present in the crystal lattice. Thus, the dioxo-V^V center exhibits a distorted trigonal-bipyramidal geometry (the *trans* angle is 156.8°), with both the oxo groups and the imine nitrogen donors occupying the basal plane. The basal plane accommodates the vanadium center without any deviation. An ORTEP view of the complex is shown in Figure 3, while crystallographic data are given in Table 1 and some selected bond lengths and angles are given in Table 2. All the metric data are well within the expected ranges and are consistent with the reported values for similar coordinations.[10] In the complex, the saccharide and aromatic moieties are arranged in a *trans* geometry with respect to the C=N bond. The dihedral angles of the saccharide moiety revealed a β-anomeric form, as was also indicated by the proton NMR study. In the solid state, both the six-membered rings of the saccharide moiety, i.e. the pyranose and the 4,6-protected part, were found to adopt a chair conformation.

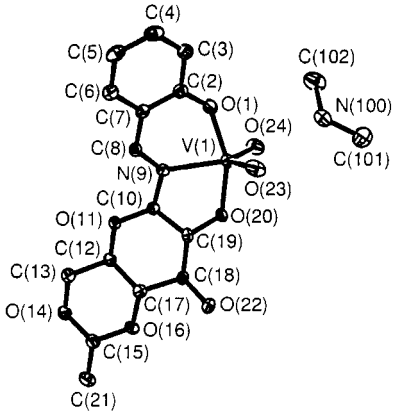

Figure 3. Molecular structure of **$[VO_2(HL^1)](Me_2NH_2)$**; thermal ellipsoids are drawn at a 50% probability level using ORTEP

Each NH group of the dimethylammonium ion is involved in one strong hydrogen bond interaction. One of the N−H bonds exhibits an additional weak interaction. These N−H protons are accepted by the oxo groups of the vanadium center (V=O) and 2-O of the saccharide moiety; 3-OH of the saccharide moiety acts as a hydrogen donor towards a second V=O group, exhibiting a strong O−H···O interaction.

Table 1. Summary of crystallographic data and parameters for $[VO_2(HL^1)](Me_2NH_2)$, $[MoO_2(HL^1)(MeOH)]MeOH$, and $[\{UO_2(HL^2)\}_2](EtOH)_2(H_2O)_2$

	$[VO_2(HL^1)](Me_2NH_2)$	$[MoO_2(HL^1)\ (MeOH)]MeOH$	$[\{UO_2(HL^2)\}_2](EtOH)_2(H_2O)_2$
Empirical formula	$C_{17}H_{25}N_2O_8V$	$C_{17}H_{25}MoNO_{10}$	$C_{36}H_{54}N_2O_{22}U_2$
Molecular mass	436.33	499.32	1342.87
T [K]	173(2)	173(2)	173(2)
Crystal system	orthorhombic	orthorhombic	hexagonal
Space group	$P2_12_12_1$	$P2_12_12_1$	$P6_2$
Cell constants			
a [Å]	6.4505(2)	7.156(1)	18.224(1)
b [Å]	10.0618(3)	14.202(1)	18.224(1)
c [Å]	29.7295(11)	19.325(1)	11.843(1)
γ [°]	–	–	120
V [Å^3]	1929.6(1)	1964.0(3)	3406.3(4)
Z	4	4	3
D [Mg/m^3]	1.502	1.689	1.964
Max./min. transmission	0.9460, 0.8495	0.8397, 0.6311	0.3760, 0.3379
Total reflections	7060	9744	18574
Unique reflections	3348 (R_{int} = 0.0318)	3400 (R_{int} = 0.0194)	3565 (R_{int} = 0.0548)
Parameters	265	273	263
Final R [$I > 2\sigma(I)$]	0.0328	0.0180	0.0463
R_w	0.0677	0.0490	0.0944

Table 2. Selected bond lengths [Å] and angles [°] for **$[VO_2(HL^1)](Me_2NH_2)$**

V(1)−O(23)	1.617(2)	V(1)−O(24)	1.626(2)
V(1)−O(20)	1.915(2)	V(1)−O(1)	1.930(2)
V(1)−N(9)	2.166(2)	O(1)−C(2)	1.314(3)
C(2)−C(7)	1.408(4)	C(7)−C(8)	1.419(4)
C(8)−N(9)	1.283(3)	N(9)−C(10)	1.448(3)
C(10)−O(11)	1.411(3)	C(10−C(19)	1.520(3)
O(11)−C(12)	1.411(3)	C(12)−C(17)	1.533(3)
C(17)−C(18)	1.519(3)	C(18)−O(22)	1.415(3)
C(18)−C(19)	1.514(3)	C(19)−O(20)	1.412(3)
O(23)−V(1)−O(24)	110.0(1)	O(23)−V(1)−O(20)	98.4(1)
O(23)−V(1)−O(1)	96.9(1)	O(23)−V(1)−N(9)	119.4(1)
O(24)−V(1)−O(20)	95.8(1)	O(24)−V(1)−O(1)	95.4(1)
O(24)−V(1)−N(9)	130.6(1)	O(20)−V(1)−O(1)	156.8(1)
O(20)−V(1)−N(9)	77.7(1)	O(1)−V(1)−N(9)	79.5(1)
V(1)−O(1)−C(2)	134.8(2)	O(1)−C(2)−C(7)	122.8(2)
C(2)−C(7)−C(8)	120.4(2)	C(7)−C(8)−N(9)	124.0(2)
C(8)−N(9)−V(1)	129.8(2)	C(8)−N(9)−C(10)	120.3(2)
N(9)−C(10)−C(19)	103.6(2)	N(9)−C(10)−O(11)	113.1(2)
C(10)−O(11)−C(12)	106.8(2)	O(11)−C(12)−C(17)	111.0(2)
C(12)−C(17)−C(18)	111.5(2)	C(17)−C(18)−O(22)	107.8(2)
C(17)−C(18)−C(19)	107.6(2)	O(22)−C(18)−C(19)	112.7(2)
C(18)−C(19)−O(20)	114.3(2)	C(18)−C(19)−C(10)	112.6(2)
C(10)−C(19)−O(20)	103.6(2)	C(19)−O(20)−V(1)	114.5(1)
C(10)−N(9)−V(1)	109.3(2)		

In addition, there are at least five C−H···O-type intermolecular interactions, for which the metric data are well within the ranges reported for such interactions in the literature.[11] The CH groups in these arise from phenyl, 3-H of saccharide, and both the methyl groups of the countercation. The acceptor oxygen atoms for these interactions are ether oxygen atoms, 2- and 3-O of the saccharide moiety, the phenolic oxygen atom, and V=O. Thus, in the lattice, each molecule is connected to four other neighbouring molecules through weak interactions, thereby forming a three-dimensional network.

Molecular and Crystal Structures of $MoO_2(HL^1)$

Slow diffusion of methanol into a concentrated solution of the complex in DMSO resulted in single crystals in the monoclinic space group. Even in this case, the ligand moiety acts as a tridentate dianion bound to a *cis*-MoO_2 unit, giving rise to one five- and one six-membered chelate, similar to the situation observed in the case of the vanadium complex. The sixth coordination site is occupied by MeOH and an additional MeOH molecule is present in the lattice. Both the molybdenum mixed-ligand complexes reported in the literature were derived from the simple protected saccharide 1,2:5,6-di-*O*-isopropylidene-D-glucofuranose.[12,13] While the complex reported by Floriani was *cis*-dioxo−Mo^{VI}, that reported by McCleverty was non-oxo−Mo^{VI}; in both the cases the saccharide acts as a monodentate ligand. To the best of our knowledge, the present structure is the first example of one in which a saccharide-based Schiff-base ligand is complexed with oxo−Mo^{VI} that has been established by single-crystal X-ray diffraction analysis. An ORTEP view of the complex is shown in Figure 4 and some selected bond lengths and bond angles are given in Table 3. All the values are consistent with earlier reports for similar coordination.[14] The crystallographic studies clearly indicate a highly distorted octahedral geometry around the molybdenum center, with the saccharide derivative binding meridionally and the metal ion deviating from the mean plane formed by O1 (phenolic), N9 (imine), O17 (saccharide 2-O), and O30 (Mo=O) by 0.305(1) Å. The *trans* angles range from 150.9(1) to 167.2(1)° and all the other angles from 75 to 107°. The remaining binding features are similar to those of the *cis*-VO_2^+ structure reported herein. The crystal structure of the Mo complex also revealed the presence of the

β-anomeric form of the saccharide moiety based on the dihedral angles. Both the six-membered rings of the saccharide moiety were found to adopt a chair conformation.

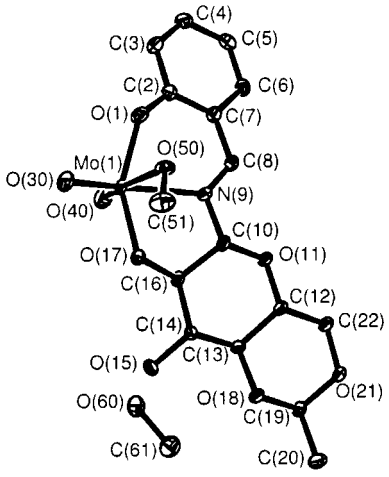

Figure 4. Molecular structure of **[MoO_2(HL^1)(MeOH)]MeOH**; thermal ellipsoids are drawn at a 50% probability level using ORTEP

Table 3. Selected bond lengths [Å] and angles [°] for **[MoO_2(HL^1)(MeOH)]MeOH**

Mo(1)−O(30)	1.704(1)	Mo(1)−O(40)	1.700(2)
Mo(1)−O(17)	1.944(1)	Mo(1)−O(1)	1.958(2)
Mo(1)−O(50)	2.368(2)	Mo(1)−N(9)	2.292(2)
O(1)−C(2)	1.343(3)	C(2)−C(7)	1.420(3)
C(7)−C(8)	1.448(3)	C(8)−N(9)	1.280(3)
N(9)−C(10)	1.444(2)	C(10)−C(16)	1.519(3)
C(10)−O(11)	1.418(2)	O(11)−C(12)	1.437(2)
C(12)−C(13)	1.528(3)	C(13)−O(18)	1.436(2)
C(13)−C(14)	1.523(3)	C(14)−O(15)	1.420(2)
C(14)−C(16)	1.527(2)	C(16)−O(17)	1.418(2)
O(40)−Mo(1)−O(30)	107.1(1)	O(40)−Mo(1)−O(17)	98.2(1)
O(40)−Mo(1)−O(1)	96.4(1)	O(40)−Mo(1)−O(50)	167.2(1)
O(40)−Mo(1)−N(9)	91.5(1)	O(30)−Mo(1)−O(17)	98.5(1)
O(30)−Mo(1)−O(1)	101.2(1)	O(30)−Mo(1)−O(50)	85.5(1)
O(30)−Mo(1)−N(9)	161.2(1)	O(17)−Mo(1)−O(1)	150.9(1)
O(17)−Mo(1)−O(50)	82.0(1)	O(17)−Mo(1)−N(9)	75.5(1)
O(1)−Mo(1)−O(50)	78.3(1)	O(1)−Mo(1)−N(9)	79.0(1)
O(50)−Mo(1)−N(9)	76.1(1)	Mo(1)−O(1)−C(2)	132.2(1)
O(1)−C(2)−C(7)	122.7(2)	C(2)−C(7)−C(8)	122.3(2)
C(7)−C(8)−N(9)	123.2(2)	C(8)−N(9)−Mo(1)	128.1(1)
C(8)−N(9)−C(10)	122.3(2)	N(9)−C(10)−O(11)	112.9(2)
N(9)−C(10)−C(16)	104.8(2)	Mo(1)−N(9)−C(10)	109.4(1)
C(16)−C(10)−O(11)	112.6(2)	C(10)−O(11)−C(12)	107.2(1)
O(11)−C(12)−C(13)	110.5(2)	C(12)−C(13)−O(18)	108.0(2)
O(18)−C(13)−C(14)	110.1(2)	C(12)−C(13)−C(14)	110.7(2)
C(13)−C(14)−O(15)	109.7(2)	C(13)−C(14)−C(16)	105.9(2)
O(15)−C(14)−C(16)	111.1(2)	C(14)−C(16)−O(17)	112.2(2)
C(16)−O(17)−Mo(1)	115.6(1)	C(14)−C(16)−C(10)	110.7(2)
O(17)−C(16)−C(10)	106.1(2)		

As a result of the extensive intermolecular involvement of both the free and bound MeOH units in the molybdenum compound, the lattice exhibits a layered structure (Figure 5), in which extended motifs, having intermolecular O−H···O and C−H···O-type interactions, are present. Both the lattice CH_3OH and 3-OH of the saccharide moiety connect the molecules present in the lattice through intermolecular O−H···O-type interactions, where the OH groups of both these moieties are involved in two such interactions by acting as both hydrogen donors and hydrogen acceptors. Thus, in effect, the molecules in the lattice are connected through zig-zag-type O−H···O interactions, as shown in Figure 6a. Similarly, the bound methanol unit is also involved in two intermolecular H-bonds, one O−H···O-type and one C−H···O-type interaction, acting as a hydrogen donor in both cases. The acceptors in these two cases are Mo=O and 6-O of the saccharide. The (metal-bound methanol)C−H···O=Mo-type interaction results in the formation of a linear chain of complex units connecting the layers, as shown in Figure 6b. Perpendicular to this chain, Ar−C−H···O=Mo type interactions extend by a connection of the molecules present in each layer, as shown in Figure 6c. Thus, the lattice consists of layers of molybdenum compounds, these being connected through extensive H-bond interactions. Furthermore, in each layer, the molecules are interconnected through H-bond interactions.

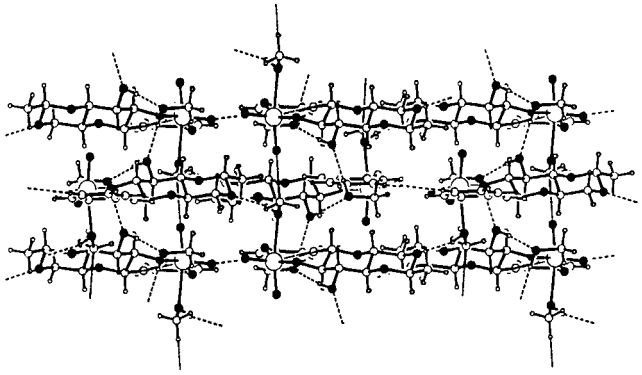

Figure 5. Layers of molecules in the lattice of the complex **[MoO_2(HL^1)(MeOH)]MeOH**; H-bond interactions are shown by dashed lines; large, open circles: metal ions; filled circles: oxygen atoms; circles with a line: nitrogen atoms

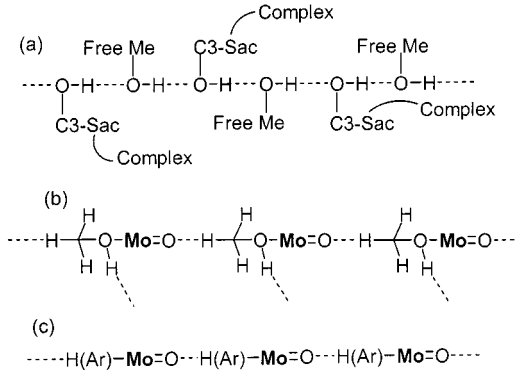

Figure 6. Weak interaction motifs present in the crystal lattice of the molybdenum complex, as determined from single-crystal X-ray diffraction analysis

Molecular and Crystal Structures of $[UO_2(HL^2)]_2$

Slow diffusion of a methanol/ethanol mixture into a concentrated solution of the complex in dichloromethane resulted in single crystals of the hexagonal system. A structural study of the product showed it to be a dinuclear *trans*-dioxo−U^{VI} complex, unlike the mononuclear complexes observed with *cis*-VO_2^+ and *cis*-MoO_2^{2+}. This is the only complex in which both the available hydroxy groups of the saccharide moiety, 2-OH and 3-OH, are involved in metal ion binding; 2-OH of the saccharide binds in its deprotonated form (2-O^-) and bridges the two metal centers giving rise to a four-membered U_2O_2 rhomb, whereas 3-OH binds to the metal ion without losing its proton. Thus, the ligand exhibits tetradentate binding plus one bridging interaction. Nevertheless, the metal-to-ligand ratio was found to be 1:1 in this complex as well. An ORTEP view of the complex is shown in Figure 7; selected bond lengths and bond angles are given in Table 4. All the values are consistent with earlier reports for a similar coordination.[15] The U_2O_2 rhomb exhibits a center of symmetry and has distances of 2.327 and 2.386 Å and angles of 113.5° and 64.9°. In addition, each asymmetric unit cell includes an ethanol and a water molecule. Even in this case, the C=N bond exhibits *trans* geometry and the saccharide moiety adopts the β-anomeric form. Both the six-membered rings of the saccharide moiety are found to adopt a chair conformation. In this complex, the *trans*-dioxo−uranium center exhibits a pentagonal-bipyramidal geometry, with the uranium ion showing almost no deviation from the basal plane [0.026(6) Å]. Thus, the *trans*-dioxo geometry of U^{VI} influences the binding characteristics of the saccharide−Schiff-base ligand.

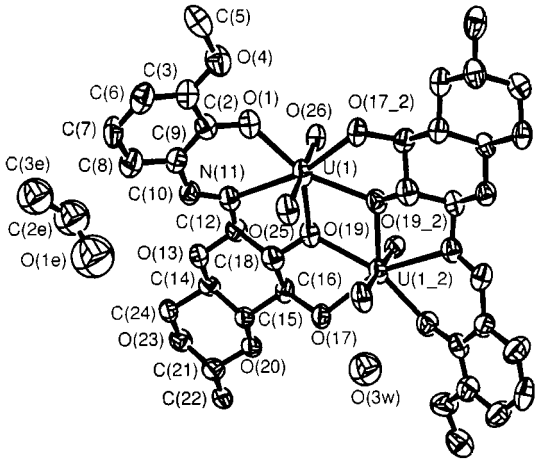

Figure 7. Molecular structure of $[\{UO_2(HL^2)\}_2](EtOH)_2(H_2O)_2$; thermal ellipsoids are drawn at a 40% probability level using ORTEP

Table 4. Selected bond lengths [Å] and angles [°] for $[\{UO_2(HL^2)\}_2](EtOH)_2(H_2O)_2$

U(1)−O(26)	1.752(16)	U(1)−O(25)	1.810(15)
U(1)−O(1)	2.235(8)	U(1)−O(19)	2.330(8)
U(1)−O(19_2)	2.404(8)	U(1)−O(17_2)	2.528(8)
U(1)−N(11)	2.571(9)	U(1)−U(1_2)	3.942(1)
O(1)−C(2)	1.337(14)	C(2)−C(9)	1.416(17)
C(9)−C(10)	1.480(18)	C(10)−N(11)	1.290(15)
N(11)−C(12)	1.452(15)	C(12)−O(13)	1.422(13)
C(12)−C(18)	1.494(17)	O(13)−C(14)	1.451(14)
C(14)−C(15)	1.527(16)	C(15)−C(16)	1.532(17)
C(16)−O(17)	1.466(14)	C(16)−C(18)	1.551(18)
C(18)−O(19)	1.386(14)		
O(26)−U(1)−O(25)	179.3(6)	O(26)−U(1)−O(1)	88.5(4)
O(26)−U(1)−O(19)	90.3(4)	O(26)−U(1)−O(19_2)	88.0(4)
O(26)−U(1)−O(17_2)	92.0(3)	O(26)−U(1)−N(11)	94.0(3)
O(25)−U(1)−O(1)	90.9(4)	O(25)−U(1)−O(19)	90.2(4)
O(25)−U(1)−O(19_2)	92.6(4)	O(25)−U(1)−O(17_2)	87.9(4)
O(25)−U(1)−N(11)	85.8(3)	O(1)−U(1)−O(19)	138.1(3)
O(1)−U(1)−O(19_2)	155.9(3)	O(1)−U(1)−O(17_2)	89.6(3)
O(1)−U(1)−N(11)	71.6(3)	O(19)−U(1)−O(19_2)	65.7(3)
O(19)−U(1)−O(17_2)	132.3(3)	O(19)−U(1)−N(11)	66.7(3)
O(19_2)−U(1)−O(17_2)	66.8(3)	O(19_2)−U(1)−N(11)	132.4(3)
O(17_2)−U(1)−N(11)	160.1(3)	U(1)−O(19)−U(1_2)	112.7(3)
C(2)−O(1)−U(1)	136.1(8)	O(1)−C(2)−C(9)	122.5(12)
N(11)−C(10)−C(9)	125.1(12)	C(10)−N(11)−C(12)	118.4(10)
O(13)−C(12)−N(11)	113.8(10)	N(11)−C(12)−C(18)	104.8(10)
C(12)−O(13)−C(14)	109.9(9)	O(13)−C(14)−C(15)	111.7(9)
O(13)−C(14)−C(24)	108.1(10)	C(15)−C(14)−C(24)	108.9(9)
O(20)−C(15)−C(14)	109.0(9)	O(20)−C(15)−C(16)	111.5(10)
C(14)−C(15)−C(16)	106.7(9)	O(17)−C(16)−C(15)	113.7(10)
O(17)−C(16)−C(18)	106.5(9)	C(15)−C(16)−C(18)	106.6(9)
O(19)−C(18)−C(16)	107.8(10)	O(19)−C(18)−C(12)	112.0(11)
C(12)−C(18)−C(16)	110.5(10)		

The *trans*-UO_2^{2+} complex crystallizes with a free ethanol and a water molecule; these do not exhibit any extended interactions, showing only discrete H-bond interactions. While the water molecule in the lattice acts as an acceptor for one O−H···O and one C−H···O interaction, the ethanol molecule acts as donor for such interactions. Thus, in the lattice, the water molecule interacts with both the ethanol molecule and 3-OH of the saccharide moiety, while the ethanol molecule is connected to 5-O of the saccharide moiety within the same molecule. In addition, the lattice contains four other C−H···O-type intermolecular interactions, which are responsible for the formation of a layer-type structure. The donors for such interactions are 4-, 5-, and 6-H of the saccharide moiety and the methoxy C−H of the salicylidene moiety, while the acceptors are 4-, 3-OH, U=O, and the phenolic O, respectively, of the neighbouring molecules in the lattice. The layer-type structure that results from these interactions is shown in Figure 8.

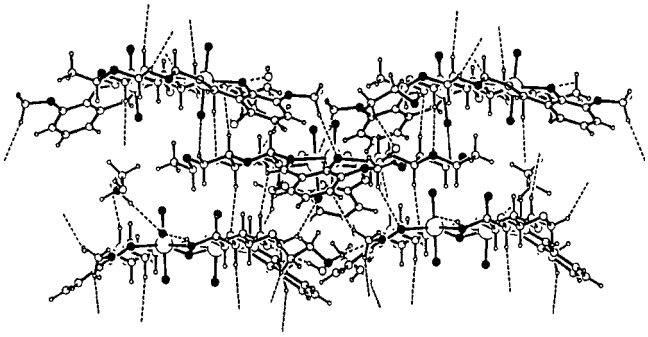

Figure 8. Layers of molecules in the lattice of the complex **[{UO_2(HL^2)}$_2$](EtOH)$_2$(H_2O)$_2$**; H-bond interactions are shown by dashed lines; large, open circles: metal ions; filled circles: oxygen atoms; circles with a line: nitrogen atoms

Conclusions

Saccharide−Schiff-base complexes of *cis*-VO_2^+, *cis*-MoO_2^{2+}, and *trans*-UO_2^{2+} have been synthesized and characterized using various analytical and spectroscopic techniques, as well as by single-crystal X-ray diffraction analysis. The NMR spectra of freshly prepared solutions in [D_6]DMSO show the saccharide moiety to be in the β-anomeric form. With *cis*-dioxo−metal ions, the ligand is tridentate, whereas with *trans*-dioxo ions it shows tetradentate coordination with an additional bridging interaction. A dianion results due to the loss of a phenolic as well as an alcoholic (2-OH of saccharide) proton. In the *trans*-UO_2^{2+} complex, 2-O^- of the saccharide moiety bridges the two uranyl centers, resulting in a dinuclear complex exhibiting a U_2O_2 rhomb, whereas 3-OH is involved in coordination without losing its proton. Metal ion binding results in the formation of one six- and two five-membered chelates. X-ray diffraction studies of the metal ion complexes revealed an increase in coordination number around the metal ion from 5 to 6 to 7 on going from *cis*-VO_2^+ to *cis*-MoO_2^{2+} to *trans*-UO_2^{2+}, corresponding to trigonal-bipyramidal, octahedral, and pentagonal-bipyramidal geometries, respectively. The dimeric structure seen in the case of the UO_2^{2+} ion complex may be attributed to the large size of the uranyl ion as well as the *trans* orientation of the oxo groups. In all the complexes, the saccharide unit adopts a chair conformation. In the lattice, weak interactions of the type O−H···O, N−H···O, and C−H···O were found to number 9, 5, and 7 for the vanadium, molybdenum, and uranium complexes, respectively. Some important features of these complexes are compared in Figure 9. As a result of these interactions, the molybdenum and uranium complexes exhibit interesting layer-type lattice structures, while the vanadium complex exhibits a three-dimensional network of hydrogen bonds. Thus, both the molecular and lattice features differ on going from *cis*-VO_2^+ to *cis*-MoO_2^{2+} to *trans*-UO_2^{2+} species, as demonstrated in this work by using saccharide-based Schiff-base ligands.

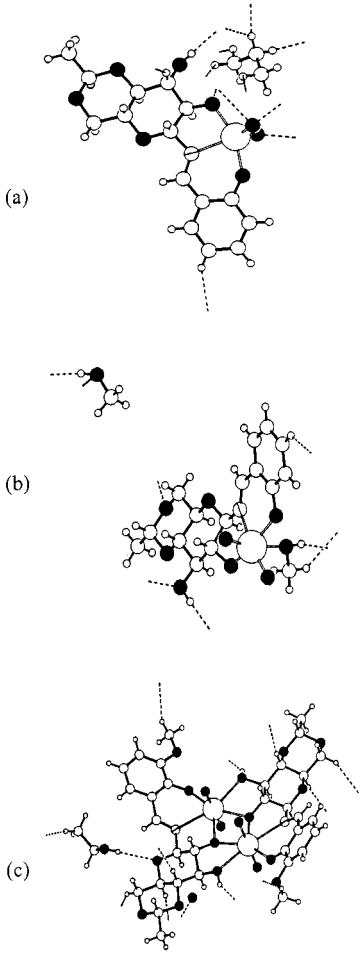

Figure 9. Coordination unit and H-bond interactions extended from each unit, as obtained from the crystal structures of (a) **[VO_2(HL^1)](Me$_2$NH_2)**, (b) **[MoO_2(HL^1)(MeOH)]MeOH**, and (c) **[{UO_2(HL^2)}$_2$](EtOH)$_2$(H_2O)$_2$**; donor/acceptor centers of H-bond interactions are indicated by dashed lines; large, open circles: metal ions; filled circles: oxygen atoms; circles with a line: nitrogen atoms

Experimental Section

General Remarks: Uranyl acetate was procured from BDH, England; the other precursors $[VO(acac)_2$ [16] and $MoO_2(acac)_2$ [17]] and 4,6-*O*-ethylidene-α-D-glucopyranose[5] and its 1-NH_2 derivative were synthesized according to reported procedures.[18] The glycosylamines $\mathbf{H_3L^1}$ and $\mathbf{H_3L^2}$ were synthesized by the condensation of 4,6-*O*-ethylidene-β-D-glucopyranosylamine with salicylaldehyde or 3-methoxysalicylaldehyde in a 1:1 ratio in ethanol, and were used after recrystallization. The solvents were procured from local sources and were purified and dried immediately prior to use. Microanalyses were carried out with a Carlo−Erba elemental analyser. − FT-IR spectra were recorded with a Nicolet Impact 400 spectrometer with samples in KBr. − UV/Vis absorption spectra were recorded with a Shimadzu UV2101PC spectrophotometer. − ^{1}H NMR spectra were recorded with Bruker Avance DRX 500 or Varian XL-300 spectrometers with samples in [D$_6$]DMSO. − FAB mass spectra were recorded with a JEOL SX 102/DA-600 mass spectrometer/data system using argon/xenon (6 kV, 10 mA) as the FAB gas and *m*-nitrobenzyl alcohol as the matrix. The accelerating voltage was 10 kV and the spectra were recorded at room temperature. − Optical rotations were measured with a JASCO model DIP-370 digital polarimeter. The abbreviations Sac, Prot, and Ar are used in the spectral assignments to denote saccharide, protecting, and aromatic groups, respectively. The ligands used and the complexes reported in this paper are shown in Scheme 1.

$[VO_2(HL^1)](Me_2NH_2)$: To a solution of $\mathbf{H_3L^1}$ (0.62 g, 2.01 mmol) in methanol (10 mL) containing dimethylamine, $VO(acac)_2$ (0.53 g, 2.00 mmol) was added and the reaction mixture was stirred at room temperature. After 10 h, oxygen was bubbled through it for 2 h and the resulting solid product was collected by filtration. The residue was washed with a small quantity of cold methanol and then with diethyl ether, and then dried in vacuo. Yield: 0.35 g (40%). − $C_{17}H_{25}N_2O_8V$ (436.33): calcd. C 46.80, H 5.77, N 6.42; found C 46.70, H 5.89, N 5.98. − ^{1}H NMR ([D$_6$]DMSO): δ = 8.50 (s, 1 H, HC=N), 7.46 (d, 1 H, ArH), 7.30 (t, 1 H, ArH), 6.67 (m, 2 H, ArH), 5.15 (br., 1 H, Sac OH), 4.75 (q, 1 H, Prot CH), 4.51 (d, 1 H, Sac 1-H), 4.18 (m, 1 H, Sac 5-H), 3.33−3.75 (m, 5 H, Sac H), 2.57 (s, 6 H, amine CH_3), 1.26 (d, 3 H, Prot CH_3). − FAB MS: *m*/*z* (%) = 391 [M + H$^+$] (95).

$[VO_2(HL^2)](Me_2NH_2)$: This compound was prepared by adopting the procedure described for **$[VO_2(HL^1)](Me_2NH_2)$**, but using $\mathbf{H_3L^2}$ (0.34 g, 1.00 mmol) and $VO(acac)_2$ (0.26 g, 0.98 mmol) in methanol (12 mL) containing dimethylamine. Yield: 0.08 g (17%). − $C_{18}H_{27}N_2O_9V$ (466.36): calcd. C 46.36, H 5.84, N 6.01; found C 46.20, H 5.56, N 6.15. − ^{1}H NMR ([D$_6$]DMSO): δ = 8.48 (s, 1 H, HC=N), 7.06 (d, 1 H, ArH), 6.93 (d, 1 H, ArH), 6.58 (t, 1 H, ArH), 5.32 (br., 1 H, Sac OH), 4.75 (q, 1 H, Prot CH), 4.51 (d, 1 H, Sac 1-H), 4.18 (m, 1 H, Sac 5-H), 3.73 (s, 3 H, $ArOCH_3$), 3.00−3.70 (m, 5 H, Sac H), 2.58 (s, 6 H, amine CH_3), 1.26 (d, 3 H, Prot CH_3). − FAB MS: *m*/*z* (%) = 418 [M − 2 H$^+$] (90).

$[MoO_2(HL^1)(H_2O)]$: To a solution of $\mathbf{H_3L^1}$ (0.62 g, 2.01 mmol) in methanol (30 mL), $MoO_2(acac)_2$ (0.65 g, 1.99 mmol) was added and the reaction mixture was stirred at room temperature for 13 h. The resulting solid product was collected by filtration, washed first with methanol and then with diethyl ether, and dried in vacuo. Yield: 0.65 g (72%). − $C_{15}H_{19}MoNO_9$ (453.25): calcd. C 39.75, H 4.22, N 3.09; found C 40.51, H 3.97, N 2.57. − ^{1}H NMR ([D$_6$]DMSO): δ = 8.55 (s, 1 H, HC=N), 7.75 (d, 1 H, ArH), 7.50 (dt, 1 H, ArH), 6.97 (t, 1 H, ArH), 6.92 (d, 1 H, ArH), 5.61 (d, 1 H, Sac OH), 4.75 (m, 2 H, Prot CH and Sac 1-H), 4.19 (m, 1 H, Sac 5-H), 3.30−3.80 (m, 5 H, Sac H), 1.27 (d, 3 H, Prot CH_3). − FAB MS: *m*/*z* (%) = 438 [M + 3 H$^+$] (40).

$[\{UO_2(HL^1)\}_2]$: This complex was prepared by adopting the procedure described for **$MoO_2(HL^1)$**, but using $\mathbf{H_3L^1}$ (0.93 g, 3.01 mmol) and $UO_2(OAc)_2{\cdot}2H_2O$ (1.27 g, 2.99 mmol) in methanol (40 mL). Yield: 1.05 g (57%). − $C_{30}H_{42}N_2O_{20}U_2$ (1226.72): calcd. C 29.37, H 3.45, N 2.28; found C 29.76, H 3.18, N 2.46. − ^{1}H NMR ([D$_6$]DMSO): δ = 9.05 (s, 1 H, HC=N), 7.50 (m, 2 H, ArH), 6.96 (d, 1 H, ArH), 6.61 (t, 1 H, ArH), 5.23 (m, 3 H, Sac OH, Sac 1-H, and Sac 3-H), 4.80 (q, 1 H, Prot CH), 4.26 (m, 1 H, Sac 5-H), 3.79 (m, 2 H, Sac H), 3.29 (m, 2 H, Sac H), 1.31 (d, 3 H, Prot CH_3). − FAB MS: *m*/*z* (%) = 1155 [M + H$^+$] (82).

$[\{UO_2(HL^2)\}_2]$: This complex was prepared by a procedure similar to that adopted for **$MoO_2(HL^1)$**, but using $\mathbf{H_3L^2}$ (1.02 g, 3.01 mmol) and $UO_2(OAc)_2{\cdot}2H_2O$ (1.27 g, 2.99 mmol) in methanol (40 mL). Yield: 1.40 g (73%). − $C_{32}H_{46}N_2O_{22}U_2$ (1286.77): calcd. C 29.86, H 3.61, N 2.17; found C 29.61, H 3.41, N 2.56. − ^{1}H NMR ([D$_6$]DMSO): δ = 9.02 (s, 1 H, HC=N), 7.13 (m, 2 H, ArH), 6.53 (t, 1 H, ArH), 5.22 (m, 3 H, Sac OH, Sac 1-H, and Sac 3-H), 4.80 (q, 1 H, Prot CH), 4.26 (m, 1 H, Sac 5-H), 3.94 (s, 3 H, $ArOCH_3$), 3.74 (m, 3 H, Sac H), 3.10−3.50 (m, 1 H, Sac H), 1.31 (d, 3 H, Prot CH_3). − FAB MS: *m*/*z* (%) = 1214 [M$^+$] (92).

X-ray Crystallography: Standard procedures were used for mounting the crystals. The diffraction data were collected with a Nonius Kappa CCD diffractometer in the φ scan + ω scan mode using Mo-K_α radiation. Single crystals of **$[VO_2(HL^1)](Me_2NH_2)$**, **$[MoO_2(HL^1)(MeOH)]MeOH$**, and **$[\{UO_2(HL^2)\}_2](EtOH)_2(H_2O)_2$** were obtained. The data were corrected for absorption by empirical methods. The structures were solved using the SHELXS-97 program package and refined using SHELXL-97.[19] The diagrams were generated using ORTEP III[20] and PLUTON-98.[21] Full-matrix least-squares refinement with anisotropic thermal parameters was used for all non-hydrogen atoms. The hydrogen atoms were treated as riding atoms with fixed thermal parameters. Other details of the data collection and structure refinement are presented in Table 1. Crystallographic data (excluding structure factors) for the structures reported in this paper have been deposited with the Cambridge Crystallographic Data Centre as supplementary publication no. CCDC-162681 for **$[VO_2(HL^1)](Me_2NH_2)$**, -162679 for **$[MoO_2(HL^1)(MeOH)]MeOH$**, -162680 for **$[\{UO_2(HL^2)\}_2](EtOH)_2(H_2O)_2$**. Copies of the data can be obtained free of charge on application to CCDC, 12 Union Road, Cambridge CB2 1EZ, UK [Fax: (internat.) + 44-1223/336-033; E-mail: deposit@ccdc.cam.ac.uk].

Acknowledgments

C. P. R. acknowledges financial support from the Council of Scientific and Industrial Research, the Department of Science and Technology, and the Board of Research in Nuclear Sciences of the Department of Atomic Energy. We thank the RSIC, CDRI Lucknow for mass spectral measurements, and Mr. R. Kuppinen for some experimental help.

[1] M. L. Sinnott, *Chem. Rev.* **1990**, *90*, 1171−1202.
[2] [2a] R. W. Gracy, E. A. Noltmann, *J. Biol. Chem.* **1968**, *243*, 5410−5419. − [2b] R. L. Root, J. R. Durrwachter, C.-H. Wong, *J. Am. Chem. Soc.* **1985**, *107*, 2997−2999. − [2c] J. Jenkins, J. Janin, F. Rey, M. Chiadmi, H. V. Tilbeurgh, I. Lasters, M. D. Maeyer, D. V. Belle, S. J. Wodak, M. Lauwereys, P. Stanssens, N. T. Mrabet, J. Snauwaert, G. Matthyssens, A.-M. Lambeir, *Biochemistry* **1992**, *31*, 5449−5458.

[3] J. A. Rendleman Jr., *Adv. Carbohydr. Chem.* **1966**, *21*, 209−271.
[4] [4a] U. Piarulli, C. Floriani, *Prog. Inorg. Chem.* **1997**, *45*, 393−429. − [4b] S. Yano, *Coord. Chem. Rev.* **1988**, *92*, 113−156. − [4c] S. Yano, K. Ohtsuka, in *Metal Ions in Biological Systems* (Eds.: H. Sigel, A. Sigel), Marcel Dekker, New York, **1996**, vol. 32, p. 27−60. − [4d] D. M. Whitfield, S. Stojkovski, B. Sarkar, *Coord. Chem. Rev.* **1993**, *122*, 171−225. − [4e] R. P. Bandwar, C. P. Rao, *Curr. Sci.* **1997**, *72*, 788−796. − [4f] Y. E. Alekseev, A. D. Garnovskii, Y. A. Zhdanov, *Russ. Chem. Rev.* **1998**, *67*, 649−669. − [4g] B. Gyurcsik, L. Nagy, *Coord. Chem. Rev.* **2000**, *203*, 81−149, and references therein.
[5] A. K. Sah, C. P. Rao, P. K. Saarenketo, E. K. Wegelius, K. Rissanen, E. Kolehmainen, *J. Chem. Soc., Dalton Trans.* **2000**, 3681−3687.
[6] R. M. Silverstein, G. C. Bassler, T. C. Morrill, *Spectrometric Identification of Organic Compounds*, 5th ed., John Wiley, New York, **1991**, p. 221−221.
[7] S. J. Angus-Dunne, R. J. Batchelar, A. S. Tracy, F. W. B. Einstein, *J. Am. Chem. Soc.* **1995**, *117*, 5292−5296.
[8] B. Zhang, S. Zhang, K. Wang, *J. Chem. Soc., Dalton Trans.* **1996**, 3257−3263.
[9] K. K. Rajak, S. P. Rath, S. Mondal, A. Chakravorty, *Inorg. Chem.* **1999**, *38*, 3283−3289.
[10] [10a] G. Asgedom, A. Sreedhara, J. Kivikoski, J. Valkonen, C. P. Rao, *J. Chem. Soc., Dalton Trans.* **1995**, 2459−2466. − [10b] G. Asgedom, A. Sreedhara, J. Kivikoski, J. Valkonen, E. Kolehmainen, C. P. Rao, *Inorg. Chem.* **1996**, *35*, 5674−5683.
[11] G. R. Desiraju, T. Steiner, *The Weak Hydrogen Bond in Structural Chemistry and Biology*, Oxford Science Publications, Oxford, **1999**, p. 29−121.
[12] A. Wlodarczyk, S. S. Kurek, M. A. J. Moss, M. S. Tolley, A. S. Batsanov, J. A. K. Howard, J. A. McCleverty, *J. Chem. Soc., Dalton Trans.* **1993**, 2027−2036.
[13] U. Piarulli, D. N. Williams, C. Floriani, G. Gervasio, D. Viterbo, *J. Chem. Soc., Dalton Trans.* **1995**, 3329−3334.
[14] [14a] C. P. Rao, A. Sreedhara, P. V. Rao, M. B. Verghese, K. Rissanen, E. Kolehmainen, N. K. Lokanath, M. A. Sridhar, J. S. Prasad, *J. Chem. Soc., Dalton Trans.* **1998**, 2383−2393.
[15] [15a] P. V. Rao, C. P. Rao, A. Sreedhara, E. K. Wegelius, K. Rissanen, E. Kolehmainen, *J. Chem. Soc., Dalton Trans.* **2000**, 1213−1218. − [15b] P. Thuéry, M. Nierlich, J. Vicens, B. Masci, *J. Chem. Soc., Dalton Trans.* **2001**, 867−874.
[16] R. A. Rowe, M. M. Jones, *Inorg. Synth.* **1957**, *5*, 113−115.
[17] M. C. Chakravorti, D. Bandyopadhyay, *Inorg. Synth.* **1992**, *29*, 129−134.
[18] K. Linek, J. Alfoldi, M. Durindova, *Chem. Pap.* **1993**, *47*, 247−250.
[19] G. M. Sheldrick, *SHELX-97 − Programs for Crystal Structure Analysis (Release 97−2)*, Institüt für Anorganische Chemie der Universität, Tammannstrasse 4, Göttingen, Germany, **1998**.
[20] M. N. Burnett, C. K. Johnson, *ORTEP III*, Report ORNL-6895, Oak Ridge National Laboratory, Oak Ridge, TN, **1996**.
[21] A. L. Spek, *Acta Crystallogr., Sect. A* **1990**, *46*, C34.

Received April 23, 2001
[I01141]